Supplementary Information (SI) for Journal of Materials Chemistry A.

# Supporting Information

# Unlocking $C_{3-4}$ Products in CO Electroreduction via One-Step Square-Ring Coupling on $Cu_4$-Embedded Carbon Nitride

**Dewei Zhang[1], Shengluo Ma[1], Yunwen Wu[2], Wei Li[3], Shenghong Ju[1, 2, *]**

[1] China-UK Low Carbon College, Shanghai Jiao Tong University, Shanghai, 201306, China

[2] Materials Genome Initiative Center, School of Material Science and Engineering, Shanghai Jiao Tong University, Shanghai 200240, China

[3] Institute for Materials and Processes, School of Engineering, The University of Edinburgh, Edinburgh EH9 3FB, Scotland, U.K.

---

[*] Corresponding author: shenghong.ju@sjtu.edu.cn.

## COMPUTATIONAL METHODS

The adsorption energy ($\Delta E_a$) of CO molecules on substrate were obtained by

$$\Delta E_a\left({}^*nCO\right) = (E\left({}^*nCO\right) - E_{sub} - nE(CO))/n\# \ (1)$$

where $n$ is the number of CO molecules, $E\left({}^*nCO\right), E_{sub}, E(CO)$ correspond to the total energies of CO molecules adsorbed on substrate, substrate and a free CO molecule in gas phase.

The Gibbs free energy ($\Delta G$)[1] was defined as

$\Delta G = \Delta E - T\Delta S + \Delta ZPE + \Delta G_U + \Delta G_{pH}\# \ (2)$

where $\Delta E$ is the charge of total energy of each state, entropy corrections $(T\Delta S)$ and zero-point energy $(\Delta ZPE)$ are calculated based on vibration analysis, all free energies are at 298.15 K, and the $\Delta S$ of CO, $H_2$, $H_2O$ and $C_{3/4}$ products were obtained from the NIST database[2]. $\Delta G_U =- neU$ is the free energy contributed by electrode potential, where $n$ is the number of electrons transferred, $e$ is the amount of charge, and $U$ is the applied potential. $\Delta G_{pH} = 2.303 * k_B T * pH$ represents the influence of the pH value[3]. Moreover, we used the computational hydrogen electrode (CHE) method.[3]

The limiting potential $(U_L)$ in full reaction path was based on

$$U_L =- \frac{\Delta G_{PDS}}{e}\# \ (3)$$

where $\Delta G_{PDS}$ is the free energy of the potential-determining step (PDS).

The charge density difference (Δρ) is calculated as

$$\Delta \rho \ = \ \rho(sub - CO) - \rho(sub) - \rho(CO)\# \ (4)$$

where $\rho(sub - CO)$and ρ(sub) represent the charge density of the substrates with and without CO absorbed, respectively, and $\rho(CO)$ represent the charge density of 1-4 CO molecules as the absorbed.

**Table S1.** 1-4 CO adsorbed at the substrate possible adsorption sites to obtain the ideal configuration, the sites are related to Figure. 1a, the adsorption energy of each atom and average C=O bond lengths are recorded.

| | Symbol | Note | Adsorption energy of each atom (eV) | Average distance of C=O | Ideal configuration |
|---|---|---|---|---|---|
| C1 | 🟢 | 1-top | -0.79 | 1.162 | |
| | 🟣 | 1-bridge | ×① | | |
| | 🔵 | 1-centroid | -1.59 | 1.247 | √ |
| C2 | 🟢–🟢 | 2-top-adjacent | ×② | | |
| | 🟣–🟣 | 2-top-diagonal | -0.71 | 1.160 | |
| | 🔵–🔵 | 2-bridge | -1.13 | 1.192 | √ |
| C3 | △ | 3-top | ×③ | | |
| | △ | 2-top-1-bridge | -0.96 | 1.168 | |
| | △ | 1-top-2-bridge | -0.94 | 1.178 | |
| | △ | 3-bridge | -1.00 | 1.188 | √ |
| C4 | □ | 4-top | -0.79 | 1.158 | |
| | □ | 4-bridge | -0.84 | 1.188 | √ |

① The initial structure of 1-bridge is optimized to 1-centroid.

② The initial structure of 2-top-adjacent is optimized to 2-bridge.

③ The initial structure of 3-top is optimized to 1-top-2-bridge.

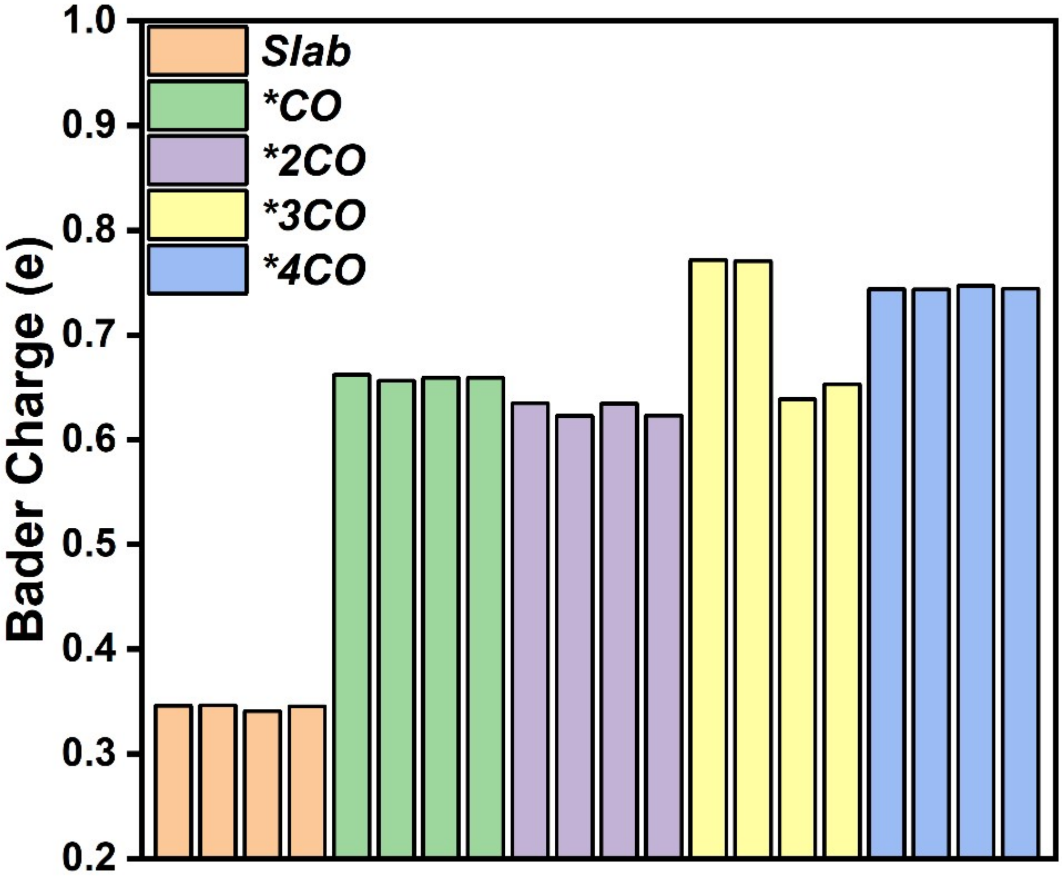

**Figure S1.** Change in Bader charge of four Cu atoms in the catalyst upon adsorption of 0-4 CO molecules.

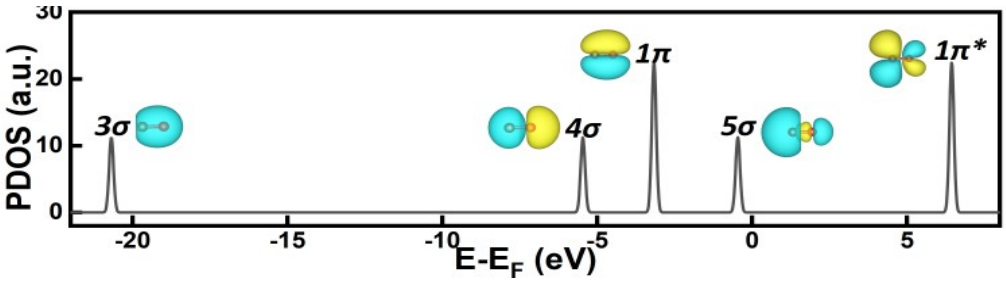

**Figure S2.** Molecular orbitals of free CO molecule, and the computed partial density of states.

**Table S2.** The thermodynamic data for the molecules considered in this paper. ((T = 298.15 K, P = 1 bar)

| Molecules | E (eV) | ZPE (eV) | TS (eV) | G (eV) |
|---|---|---|---|---|
| $H_2$ (g) | -6.77 | 0.29 | 0.40 | -6.88 |
| $H_2O$ (l) | -14.23 | 0.57 | 0.58 | -14.24 |
| CO (g) | -14.79 | 0.14 | 0.61 | -15.26 |
| $CH_4$ (g) | -24.07 | 1.19 | 0.58 | -23.45 |
| $CH_3OH$ (l) | -30.26 | 1.36 | 0.74 | -29.64 |
| $CH_3CHCH_2$ (g) | -48.80 | 2.12 | 0.82 | -47.50 |
| $CH_3CH_2CH_2OH$ (l) | -63.59 | 2.88 | 1.00 | -61.71 |
| $CH_2CHCHCH_2$ (g) | -57.19 | 2.28 | 0.86 | -55.77 |
| $CH_2CH_2CH_2CH_2$ (g) | -65.22 | 2.94 | 0.82 | -63.10 |
| $CH_3CH_2CHCH_2$ (g) | -65.30 | 2.87 | 0.95 | -63.39 |
| $CH_3CH_2CH_3CH_2OH$ (l) | -80.19 | 3.62 | 1.12 | -77.69 |

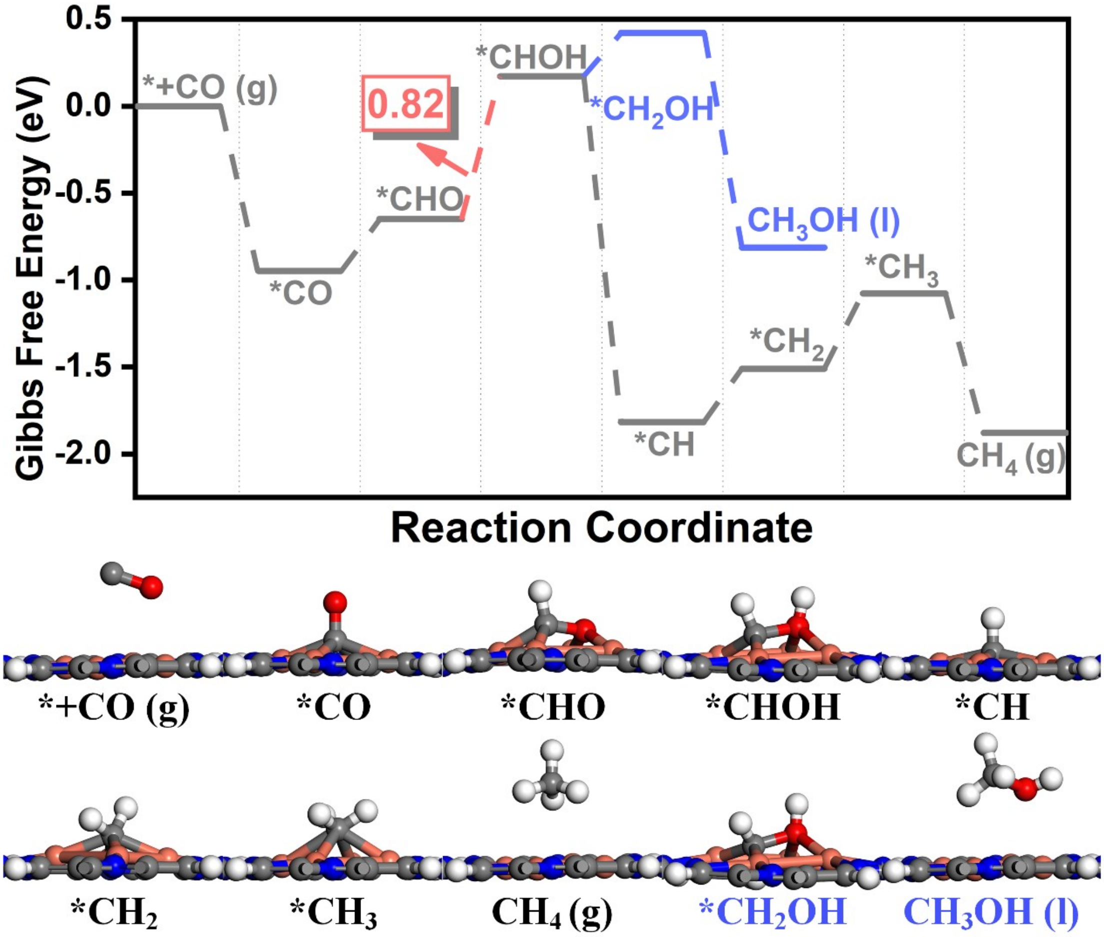

**Figure S3.** Free energy diagram and optimized structures of the CORR pathways to $CH_4$ and $CH_3OH$ on $Cu_4$-$C_5N_2H_2$.

**Table S3.** Specific values of the free energy change for each step in the generation of the $C_3$ products in $Cu_4$-$C_5N_2H_2$ shown in Figure 5, the colour coding is also consistent.

| Step | Elementary Step | ΔG (eV) |
|---|---|---|
| 1 | $3CO\ (g)+* \rightarrow *CO+*CO+*CO$ | -1.11 |
| 2 | $*CO+*CO+*CO \rightarrow *CO*CO*CO$ | 0.20 |
| 3 | $*CO*CO*CO+H^{+}+e^{-} \rightarrow COH*CO*CO$ | -0.04 |
| 4 | $*COH*CO*CO+H^{+}+e^{-} \rightarrow *COH*COH*CO$ | -0.19 |
| 5 | $*COH*COH*CO+H^{+}+e^{-} \rightarrow *COH*COH*COH$ | 0.47 |
| 6 | $*COH*COH*COH+H^{+}+e^{-} \rightarrow *C*COH*COH+H_2O$ | 0.55 |
| 7 | $*C*COH*COH+H^{+}+e^{-} \rightarrow *CH*COH*COH$ | -1.45 |
| 8 | $*CH*COH*COH+H^{+}+e^{-} \rightarrow *CH*C*COH+H_2O$ | 0.40 |
| 9 | $*CH*C*COH+H^{+}+e^{-} \rightarrow *CH*CH*COH$ | -0.84 |
| 10 | $*CH*CH*COH+H^{+}+e^{-} \rightarrow *CH*CH*C+H_2O$<br>$*CH*CH*COH+H^{+}+e^{-} \rightarrow *CH_2*CH*COH$ | 0.27<br>0.03 |
| 11 | $*CH*CH*C+H^{+}+e^{-} \rightarrow *CH*CH*CH$<br>$*CH_2*CH*COH+H^{+}+e^{-} \rightarrow *CH_2*CH*CHOH$ | -0.57<br>-0.07 |
| 12 | $*CH*CH*CH+H^{+}+e^{-} \rightarrow *CH_2*CH*CH$<br>$*CH_2*CH*CHOH+H^{+}+e^{-} \rightarrow CH_3*CH*CHOH$ | -0.45<br>0.95 |
| 13 | $*CH_2*CH*CH+H^{+}+e^{-} \rightarrow *CH_2*CH*CH_2$<br>$CH_3*CH*CHOH+H^{+}+e^{-} \rightarrow CH_3CH_2*CHOH$ | -0.25<br>-1.17 |
| 14 | $*CH_2*CH*CH_2+H^{+}+e^{-} \rightarrow CH_3*CH*CH_2$<br>$CH_3CH_2*CHOH+H^{+}+e^{-} \rightarrow CH_3CH_2CH_2OH+*$ | 0.04<br>-0.85 |
| 15 | $CH_3*CH*CH_2 \rightarrow CH_3CHCH_2+*$ | -0.46 |

**Table S4.** Specific values of the free energy change for each step in the generation of the $C_4$ products in $Cu_4$-$C_5N_2H_2$ shown in Figure 6, the colour coding is also consistent.

| Step | Elementary Step | ΔG (eV) |
|---|---|---|
| 1 | 4CO (g)+* → *CO+*CO+*CO+*CO | -0.88 |
| 2 | *CO+*CO+*CO+*CO → *CO*CO*CO*CO(□) | 0.26 |
| 3 | *CO*CO*CO*CO(□)+$H^+$+$e^-$ → *CO*COH*CO*CO | -0.30 |
| 4 | *CO*COH*CO*CO+$H^+$+$e^-$ → *CO*COH*COH*CO | 0.23 |
| 5 | *CO*COH*COH*CO+$H^+$+$e^-$ → *CO*COH*COH*COH | 0.11 |
| 6 | *CO*COH*COH*COH+$H^+$+$e^-$ → *COH*COH*COH*COH | 0.47 |
| 7 | *COH*COH*COH*COH+$H^+$+$e^-$ → *C*COH*COH*COH+$H_2O$ | 0.26 |
| 8 | *C*COH*COH*COH+$H^+$+$e^-$ → *CH*COH*COH*COH | -0.95 |
| 9 | *CH*COH*COH*COH+$H^+$+$e^-$ → *CH*C*COH*COH+$H_2O$ | 0.33 |
| 10 | *CH*C*COH*COH+$H^+$+$e^-$ → *CH*CH*COH*COH | -1.00 |
| 11 | *CH*CH*COH*COH+$H^+$+$e^-$ → *CH*CH*C*COH+$H_2O$ | 0.10 |
| 12 | *CH*CH*C*COH+$H^+$+$e^-$ → *CH*CH*CH*COH | -0.86 |
| 13 | *CH*CH*CH*COH+$H^+$+$e^-$ → *CH*CH*CH*C+$H_2O$<br>*CH*CH*CH*COH+$H^+$+$e^-$ →*$CH_2$*CH*CH*COH | 0.64<br>-0.87 |
| 14 | *CH*CH*CH*C+$H^+$+$e^-$ → *CH*CH*CH*CH<br>*CH*CH*CH*C+$H^+$+$e^-$ → *CH*CH*CH*CH(□)<br>*$CH_2$*CH*CH*COH+$H^+$+$e^-$ → *$CH_2$*CH*CH*CHOH | -1.21<br>-0.63<br>0.41 |
| 15 | *CH*CH*CH*CH+$H^+$+$e^-$ → *$CH_2$*CH*CH*CH<br>*CH*CH*CH*CH(□)+$H^+$+$e^-$ → $CH_2$*CH*CH*CH(□)<br>*$CH_2$*CH*CH*COH+$H^+$+$e^-$ → *$CH_3$*CH*CH*CHOH | -1.03<br>-0.37<br>-0.25 |
| 16 | *$CH_2$*CH*CH*CH+$H^+$+$e^-$ → *$CH_2$*CH*CH*$CH_2$<br>$CH_2$*CH*CH*CH+$H^+$+$e^-$ → $CH_2CH_2$*CH*CH(□)<br>*$CH_3$*CH*CH*CHOH+$H^+$+$e^-$ → $CH_3$*CH*$CH_2$*CHOH | 0.92<br>0.31<br>0.53 |
| 17 | *$CH_2$*CH*CH*$CH_2$ → $CH_2CHCHCH_2$+*<br>*$CH_2$*CH*CH*$CH_2$+$H^+$+$e^-$ → $CH_3$*CH*CH*$CH_2$<br>$CH_2CH_2$*CH*CH+$H^+$+$e^-$ → $CH_2CH_2CH_2$*CH(□)<br>$CH_3$*CH*$CH_2$*CHOH+$H^+$+$e^-$ → $CH_3CH_2CH_2$*CHOH | -0.59<br>-0.64<br>-0.56<br>-0.70 |
| 18 | $CH_3$*CH*CH*$CH_2$+$H^+$+$e^-$ → $CH_3CH_2CHCH_2$+*<br>$CH_2CH_2CH_2$*CH+$H^+$+$e^-$ → $CH_2CH_2CH_2CH_2$(□) +*<br>$CH_3CH_2CH_2$*CHOH+$H^+$+$e^-$ → $CH_3CH_2CH_2CH_2OH$+* | -0.69<br>-1.12<br>-1.20 |

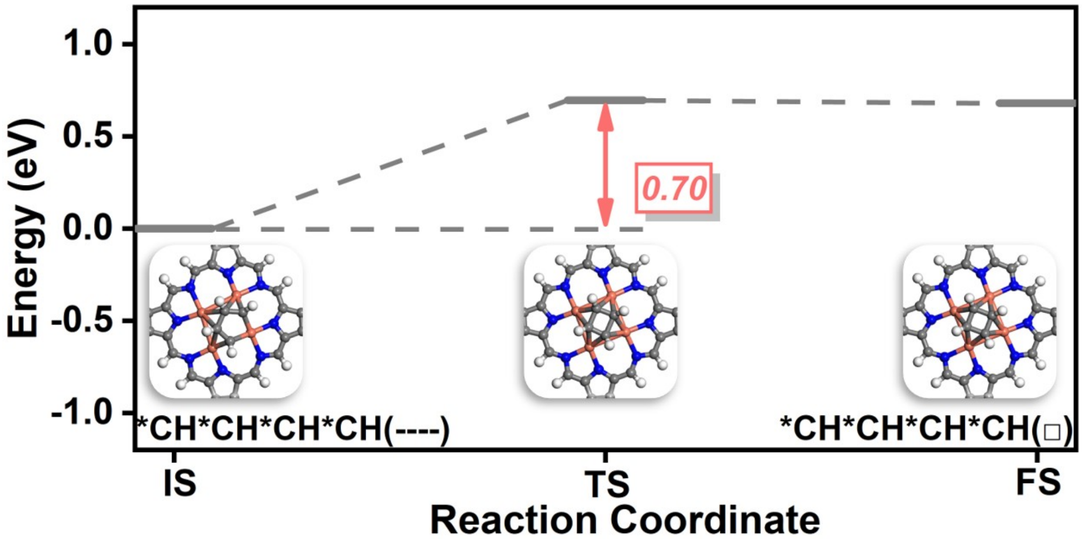

**Figure S4.** Transition state calculations of the energy change of the straight chain *CH*CH*CH*CH via C-C coupling to get the cyclic chain *CH*CH*CH*CH(□).

## Reference

[1] A.A. Peterson, F. Abild-Pedersen, F. Studt, J. Rossmeisl and J.K. Nørskov, How copper catalyzes the electroreduction of carbon dioxide into hydrocarbon fuels, Energy & Environmental Science 3 (2010) 1311-1315.

[2] R.D.J. III, NIST Computational Chemistry Comparison and Benchmark DataBase., https://cccbdb.nist.gov

[3] J.K. Norskov, J. Rossmeisl, A. Logadottir, L. Lindqvist, J.R. Kitchin, T. Bligaard and H. Jonsson, Origin of the Overpotential for Oxygen Reduction at a Fuel-Cell Cathode, Journal of Physical Chemistry B 108 (2004) 17886-17892.